Contract Information

Contract Number	N00014-03-1-0777
Title of Research	Active Control of Blade Tonals in Underwater Vehicles
Principal Investigator	Anuradha M. Annaswamy
Organization	Massachusetts Institute of Technology

The goal of this proposal is to achieve stealth through the reduction or alteration of radiated noise that produce blade tonals in underwater vehicles. The use of active control that is judiciously integrated with passive control is proposed to realize which consists of intentional articulation of suitable surfaces or boundary conditions in the vehicle so as to modify the relevant noise characteristics. By modulating additional surfaces, biological organisms appear to affect lift, drag, and related wake producing features, a combination of which may lead to a modification of the underlying acoustic characteristics. Our thesis is that by distilling some of the fundamental features of these mechanisms, and suitably accommodating them in underwater vehicles, significant changes in the noise production can be made by expending very little energy. By modulating suitable foils and components as a function of the flow-field around the vehicle at appropriate spatial locations and time-scales, the goal is achieve significant change in the gust amplitudes and resulting noise production. The aim of this proposal is therefore to determine active biomimetic control methods for reducing/altering blade tonal signatures.

Technical Section

Technical objectives

The following are the technical objectives that will help us reach the goal of tactical noise alteration:

1. Develop actuation methods for articulating tail that provide a maximum benefit of alteration of unsteady forces that produce noise while minimizing the impact on thrust loss. This will include model development, actuator design, and control design.

2. Integrate the actuator with a suitable stator model.

3. Design and implement the experiments using the above stators integrated with actuators.

4. Develop a relationship with NUWC to facilitate a follow-on study of the proposed concept for acoustic characterizations.

Technical Approach

The goal is to realize tactical noise alternation by addressing the component due to direct radiation when a propulsor rotor encounters a wake deficit from a stator. Our approach for altering/reducing this noise component is to carry out an experimental investigation where a tail-airfoil is attached to a stator, which is then suitably articulated so as to achieve desired effects further downstream. In addition, it was planned to quantify the unsteady propulsor inflow generated by passive and active stator control using both PIV (Particle Image Velocimetry) and LDV (Laser Doppler Anemometry) based techniques, PUF-simulations, and force-measurement (load cell) based techniques to corroborate the velocity measurements and the PUF simulations.

I Stator and Tail Fabrication

The first stage of our investigations was the fabrication of the active stator that will eventually be used in a real time propeller noise-control test. A life size (3" chord, 6" span) airfoil was fabricated with a 1/3 chord flapping tail section. The stator was designed to operate in either the MIT water tunnel facility or in the research water tunnel at NUWC, Newport. In these tunnels the stator would be tested at much higher Reynolds numbers, *Re*, than were previously investigated (75,000 < *Re* < 300,000). Frequency dependence of phenomena was expected to scale with the flow speed by the Strouhal number,

$$St = \frac{frequency * tail_{deflection}}{U},$$

so considerable care was taken to meet the project frequency requirements of 30 Hz. No actuators identified could meet the accelerations necessary to oscillate sinusoidally up to 30 Hz so a mechanism was designed to meet the requirements. The crank rocker mechanism pictured below converts rotation of the input link to nearly sinusoidal output, with an amplitude set by the length of the input link, which is adjustable. In this configuration the requirements for the input motor became a rotational speed of 2000 rpm at a torque of 1.2 Nm, for which a capable servo motor was easily selected. A motor controller/data acquisition board was also selected. The board is capable of controlling up to four motors in either stepper or servo configurations and has four trigger channels as well as four channels of A/D conversion. This board was selected because it will scale easily to the future task of simultaneously controlling tail articulation as well as controlling an instrumented propeller and recording data.

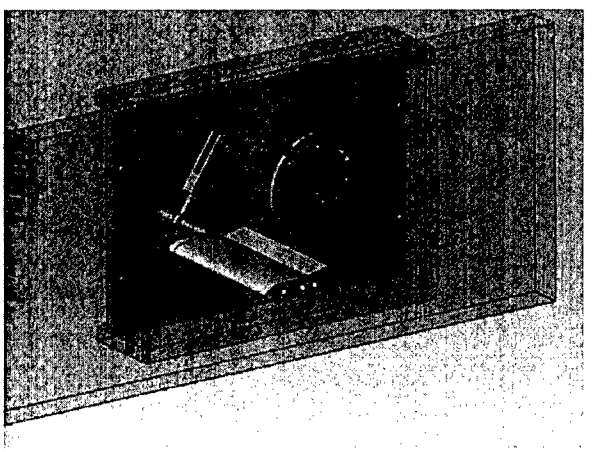

Figure 1 Structure of the crank rocker mechanism for tail articulation

In addition to the research water tunnel, NUWC made available both LDV and PIV measurement tools for use on this project (Figure 2). LDV was used to accurately measure the mean flow velocity at a single interrogation point over a large number of flapping periods, as well as spectral and turbulence intensity data. PIV was used to examine the instantaneous two dimensional plane velocities downstream of the stator. PIV data were phase averaged so that flow visualization could provide insight into the dynamic quality of the articulated wake.

II Velocity Measurements

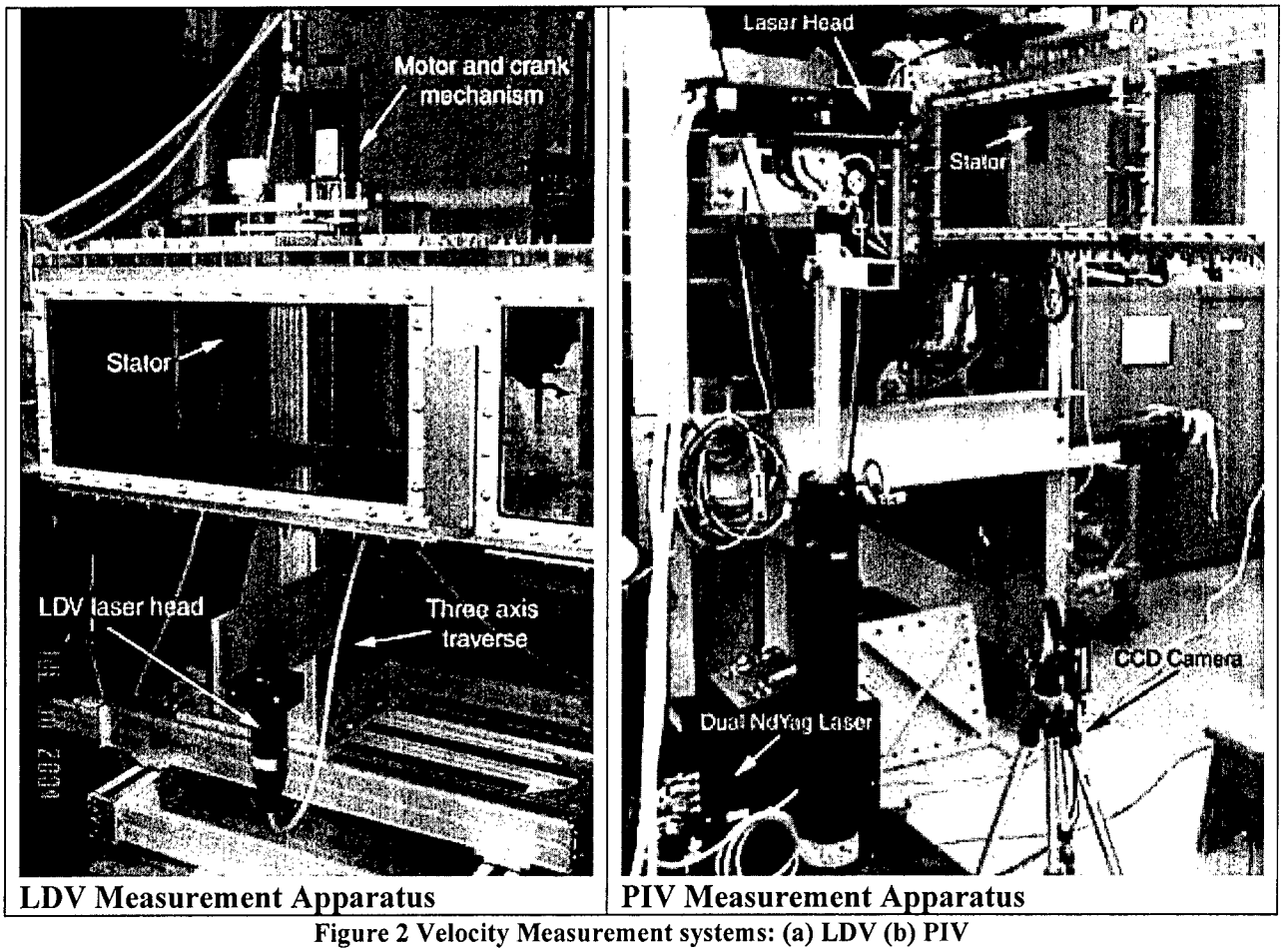

Figure 2 Velocity Measurement systems: (a) LDV (b) PIV

Because of the relatively low aspect ratio between the stator span and chord, initial LDV measurements were set up to measure the streamwise component of velocity, u or left to right in the above photo, as well as the spanwise component, w or up and down. The w component of velocity was found to be less than two percent of the freestream velocity at the midspan location, even while actively articulating the tail. Therefore, it was concluded that the two dimensional analysis of the velocity field behind the stator was sufficient to measure the effects of tail articulation. Afterwards the LDV system was realigned to measure the u and v components of velocity and a total of 120 wake profiles, including 46 transients were taken. For each wake profile, data were taken at least 25 points in the y direction, across the tunnel, one chord length downstream of the stator. The results obtained are shown and discussed below. It should be noted that all of the results reported here were obtained in experimental investigations carried out in the NUWC water tunnel.

Velocity data was averaged over at least 20 flapping periods for each individual point. In this data the effect of tail articulation can be seen quite readily. Figure 3 shows the wake changing as the tail is flapped sinusoidally at increasing frequency and with an amplitude of 10 degrees The first line, $St = 0$, corresponds to the baseline wake which has a wake depth of $\frac{u-U}{U} = 0.12$. As St increases, which is linear with frequency, and it can be seen that initially the wake deficit spreads out over a larger area, begins to lessen and finally reverses. The v component of

velocity is shown in Figure 4. It is seen that at low *St* the v component of velocity is almost zero. But in the region where the wake is reversed the v component becomes significant and anti-symmetric. This is consistent with the theory that wake profile is reversed due to the production of a thrust generating Karman vortex street.

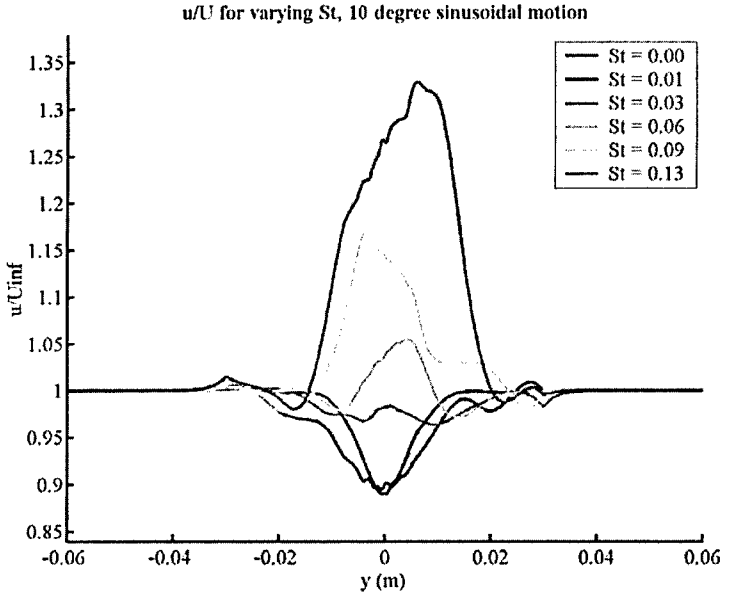

Figure 3 Effect of the flapping tail on the wake (u-component) at different St

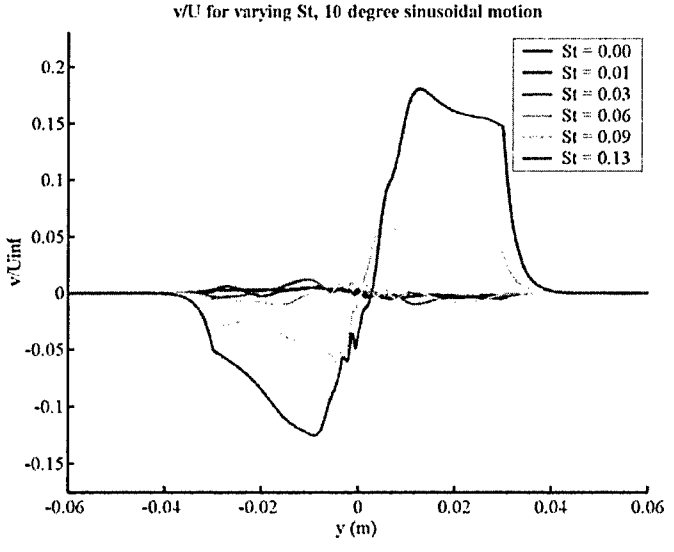

Figure 4 Effect of the flapping tail on the wake (u-component) at different St

Wake profiles like those shown above were analyzed to find the relationship between *St* and the effective coefficient of drag of the stator, C_d. Because the stator is a streamlined shape the wake deficit responsible for blade tonal noise is due mainly to surface drag, which can be thought of as a shedding into the wake of momentum lost in the boundary layer. It is assumed that far away from the stator there is an irrotational streamline around the stator, through which

no momentum is lost (see Figure 5). By examining the u velocity on control surfaces up and downstream of the stator, through which mass is conserved, the mean C_d of the stator can be estimated.

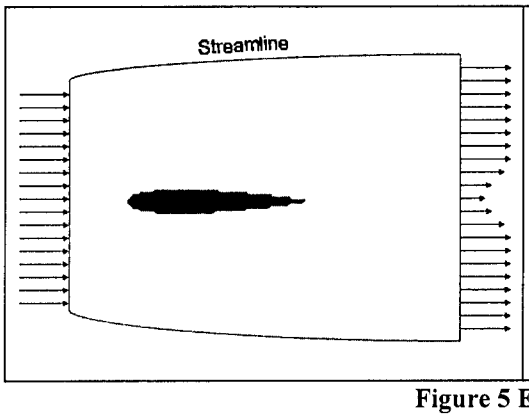

$$0 = \oint_{cs} p * u \bullet \hat{n} dA = pS\left(\int_{y\min}^{y\max} u dy - \int_{y1}^{y2} U dy\right), \text{ mass conservation}$$

$$\sum F_x = D = \oint_{cs} u * p * u \bullet \hat{n} dA = pS\left(\int_{y\min}^{y\max} u^2 - (U * u) dy\right)$$

$$C_d = \frac{D}{\frac{1}{2} pU^2 S * L} = \frac{2}{L}\int_{y\min}^{y\max}\left(\frac{u}{U}\right)^2 - \left(\frac{u}{U}\right) dy$$

Figure 5 Effect of the flapping tail on C_d

Figure 6 shows C_d plotted as a function of St, for ten degree sinusoidal flapping. At St = 0, the no flapping, C_d has a positive value of .02-.03 for each case, this is a measure of the baseline surface drag. For small St, C_d increases from the baseline case, meaning that the input energy from tail articulation is increasing the energy lost in the flow. However, after a certain threshold, approximately St = 0.01, tail articulation begins to lessen the effective C_d. At St = 0.05, C_d goes to zero, meaning that in the mean the energy input by tail articulation has exactly replaced the energy lost to drag. This is no indication of efficient drag reduction. However, because the conversion of unsteady force to radiated noise may be very efficient, the gain in noise reduction compared to the energy input for tail articulation may be large, depending on mission priorities. For larger St the wake reversal results in an increase in momentum throughout the control volume, meaning that tail articulation is producing thrust, which results in a negative value of C_d. In the mean this region is not ideal for noise reduction as the blade will experience unsteady loading of the opposite sign as it passes though the thrust producing wake. Similar relationships between C_d and St were evident for 5 and 20 degree flapping as well. Transient motions were

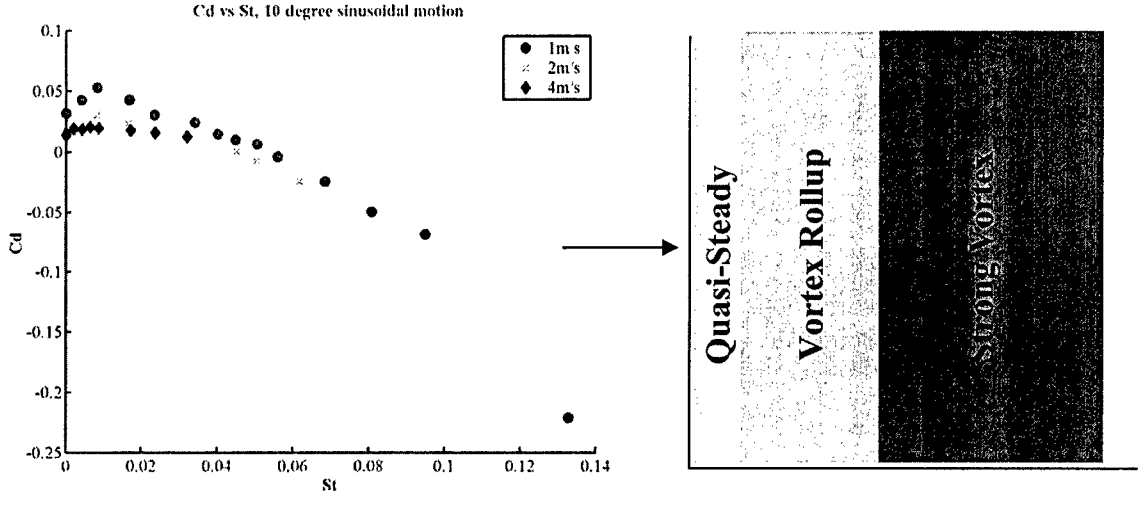

Figure 6: Plot of mean Cd as a function of St for varying speeds and the vortex regimes they correspond to.

also found to either increase and decrease C_d, however it is still unclear how to best define *St* for a transient motion.

From LDV and PIV measurements it became apparent that there were three distinct regimes of wake flow due to active articulation. The roll up of an alternating vortex sheet shed by the stator is a primary descriptor of the active wake. At low Strouhal numbers (*St*), corresponding to a high drag coefficient (*Cd*) the vortex wake was seen to move in a quasi-steady manner. At moderate *St* (corresponding to a low *Cd*) the vortex sheet was found to begin to roll up. In this region tail articulation has introduced enough energy to cancel the wake deficit created by the stator in a time-mean sense. Instantaneously, however, the wake still has strong unsteady fluctuations. At high *St* (corresponding to negative *Cd* i.e. thrust) vortex sheet roll up was seen to occur quickly resulting in a strong vortex wake. The exact relation between *Cd* and St depends on the amplitude of tail articulation and articulation profile.

To better understand the regions of interest in tail articulation, PIV measurements were taken at key *St* identified in the LDV data. Visualization of this data made the qualitative interpretation of the effect of tail articulation quite clear for different *St* ranges. Figure 7 shows the vorticity shed from the stator without tail articulation. The vorticity is shed directly downstream, dissipating rather slowly. Notice that by the sign of the vorticity the induced velocity in the center of the wake is negative, which results in a wake velocity deficit.

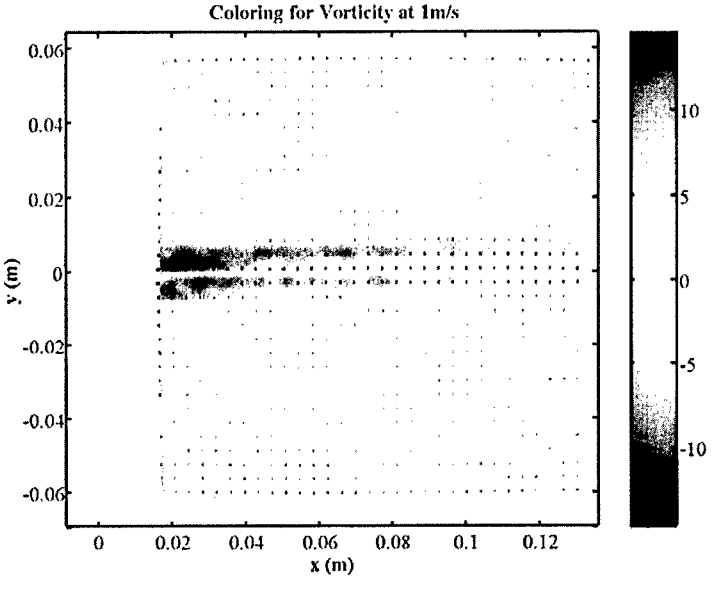

Figure 7 Wake deficit in the baseline case, at 1m/s (without any tail articulation)

Figure 8 shows a portion of the wake for tail articulation at low *St*. It is seen that the motion of the tail acts to spread the wake out, with the instantaneous vorticity shed a function of the quasi-steady circulation around the foil. This type of wake is well predicted by linear unsteady airfoil theory, such as the Theodorsen function. At the critical *St*, where C_d goes to zero, the wake is seen to be in a state of disarray (figure 9). The shed vorticity has began to roll up, as the wavelength of the shed vorticity in space is small enough that the induced velocity due to vorticity of similar signs becomes significant. While this type of results in a mean zero wake

deficit, the vortex rollup at this stage is not very repeatable. Therefore, this type of wake may not be the best suited for controlling blade tonal noise.

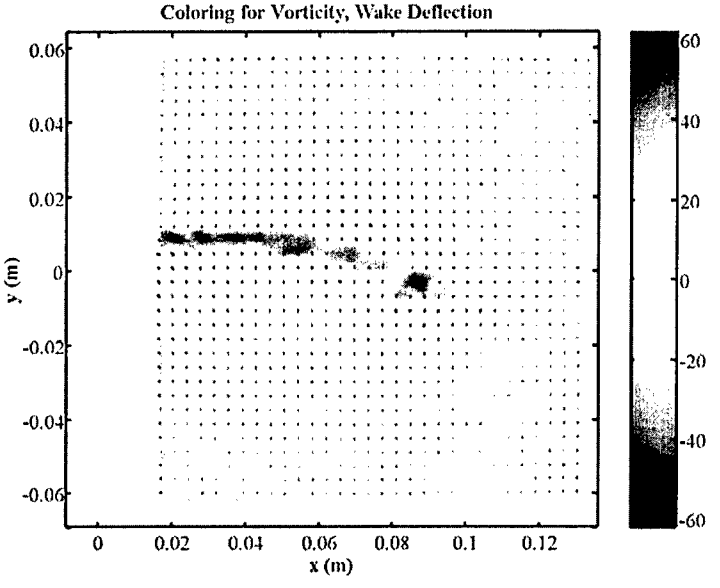

Figure 8 Wake deficit with tail articulation at low St, at 1m/s

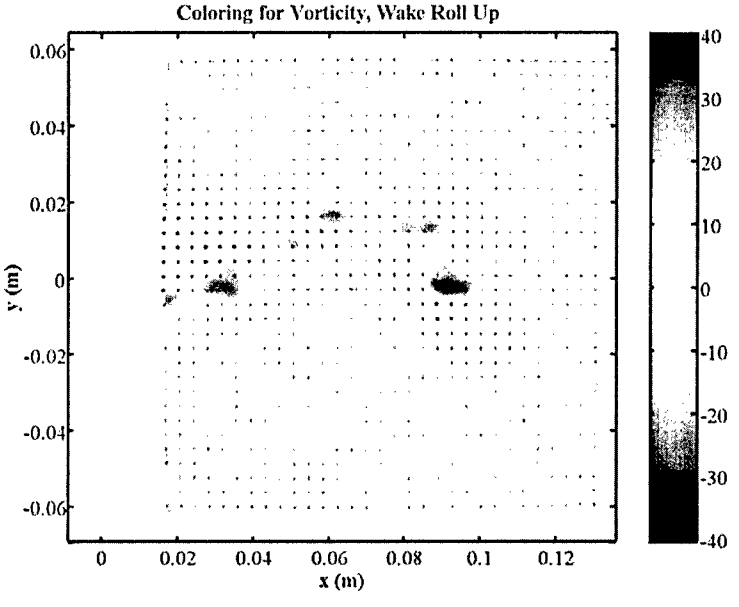

Figure 9 Wake deficit with tail articulation at the critical St, 1m/s

The final type of wake observed was that for high *St*, with significant thrust produced (Figure 10). In this type of a wake the vortex rollup is very repeatable and so might be a good candidate for controlling the reduction of blade tonal noise. However, considerable thought will have to be given to the interaction of these vortex cores with the propeller blade. This interaction is highly coupled, as the vortices and blade both induce velocity potentials on each other, and highly three dimensional when a real rotor is examined. Instantaneous wake profiles from non-sinusoidal motions show that there may be promise in using these types of motions. Figure 11-1) and 11-2) represent the wake of a tail articulation based on a $\sin(wt)^4$ profile as well as a generalized transient case with $\theta = 2\pi/3$ and $R = 1$ both with the same base period. In both cases strong repeatable vortices are formed in the wake; however their pattern is dramatically different from the sinusoidal case and from each other. If the connection between tail motion and vortex distribution can be found, then a tail motion ideal for blade tonal reduction could be inversely designed to give the ideal blade vortex interaction.

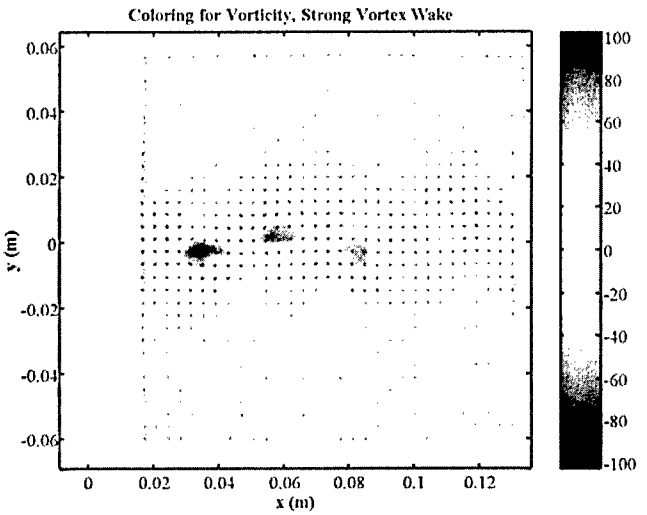

Figure 10 Wake deficit with tail articulation at high St, 1m/s

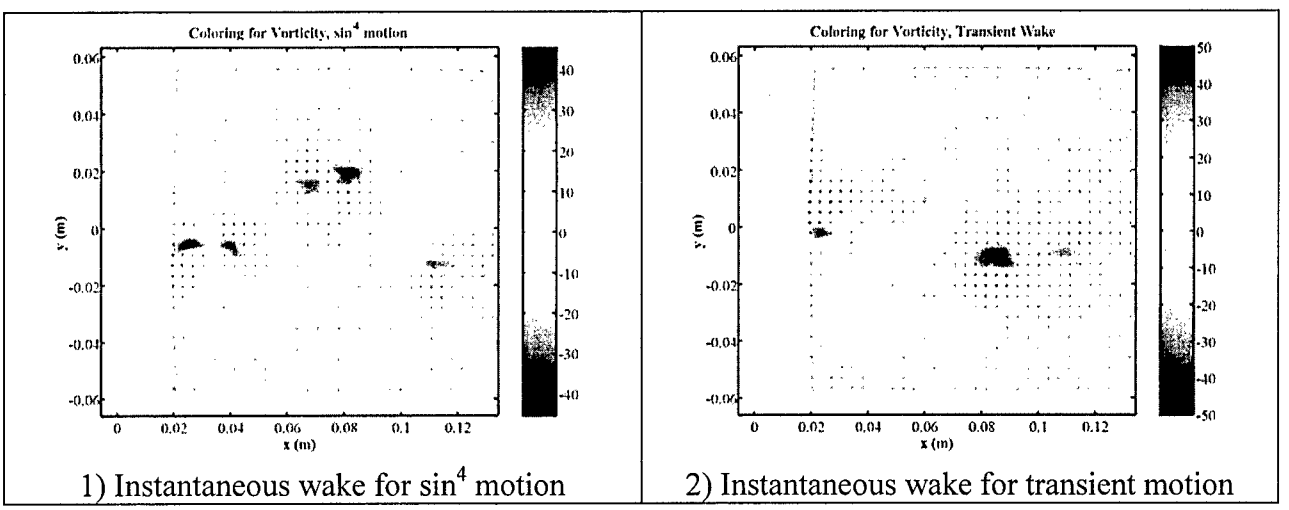

1) Instantaneous wake for $\sin^4$ motion

2) Instantaneous wake for transient motion

Figure 11 Wake profiles with sinusoidal and nonsinusoidal motion

In order to verify the effect of the wake alterations reported above, the experimental data was ported onto a proven propeller noise simulation program, the propeller unsteady force code, PUF. A suitable propeller geometry, similar to those used later in the force measurements was used in PUF simulations. The challenge for simulation will be in defining the boundary/initial conditions and in the choice of how to best represent the vortex wake in the PUF code. As a first step, only time mean wakes as shown in Figure 12 were investigated. The first wake in Figure 12 is the baseline case, while the second represents the time mean data for a thrust producing wake, in which the sign of the wake deficit is reversed.

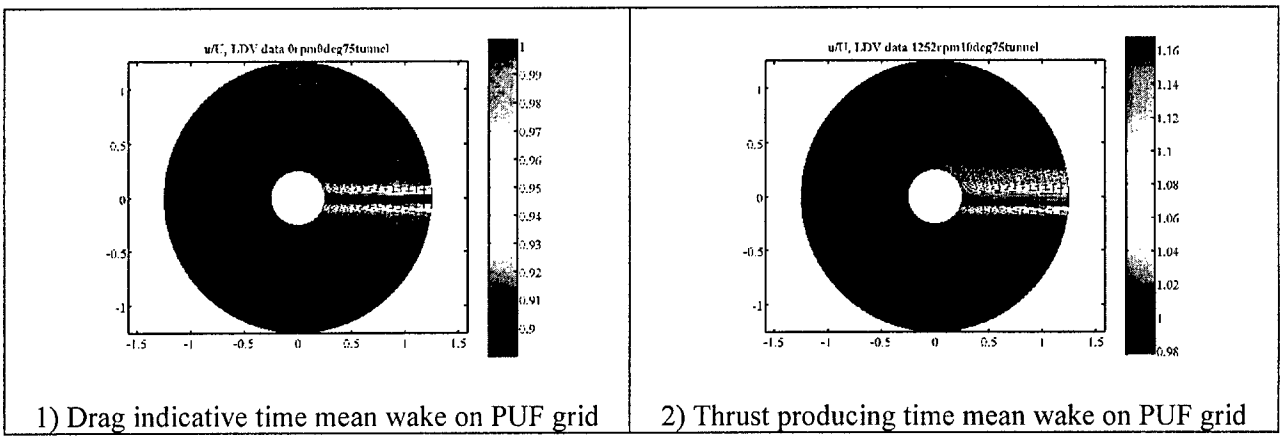

1) Drag indicative time mean wake on PUF grid

2) Thrust producing time mean wake on PUF grid

Figure 12 Time mean wakes analyzed with the PUF simulations

III. A Low-order Model

A low order model of the wake due to tail articulation was constructed which was able to replicate observed vortex sheet roll up for both sinusoidal and non-sinusoidal move profiles. This model was also able to capture the baseline wake deficit measured. 2-dimensional blade interaction was simulated using the vortex wake generated by the reduced order model of tail articulation. This simulation allowed for quick estimates of the noise reduction possible with a specific tail motion. 3D propeller unsteady force (PUF) code provided a means of calculating more accurate predictions of unsteady propeller force and noise once scenarios of interest were identified by 2D simulations.

The vorticity shed by the baseline wake and articulation tail was modeled using the following relations based on tail tip velocity and geometry: Defomomg U is stream velocity, v is tip velocity, δ is the boundary layer thickness and L is tail length, we obtain that

$$\gamma_0 = \frac{1}{2}U^2\Delta t$$

$$\gamma_{net}(t) = -\frac{UL_{tip}\Delta t}{\delta}v_{tip}(t)$$

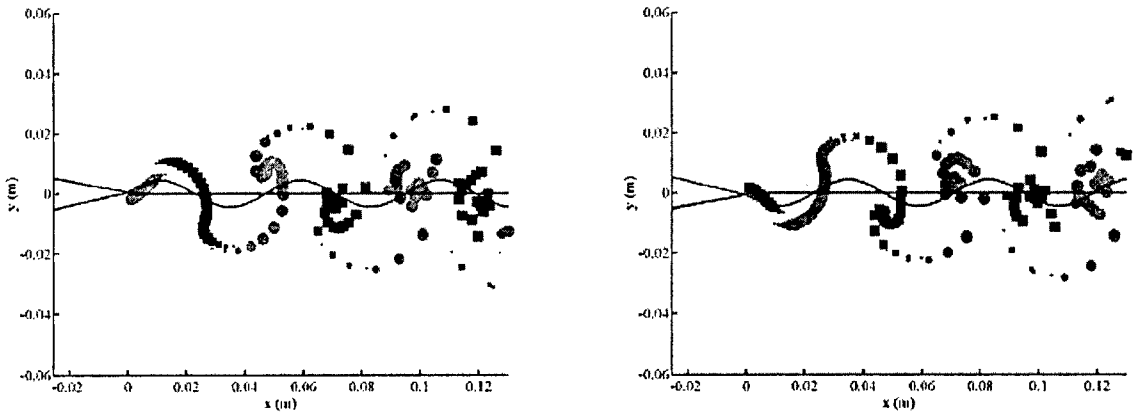

Figure 13 Reduced order wake simulation in strong vortex regime. f = 1252 rpm, A = 10 deg, U = 1 m/s, St = 0.186

Figure 13 shows an example of a strong vortex wake simulated using the reduced order model. The reduced order wake model was used in conjunction with a 2D blade-vortex interaction model (based on a Hess-Smith panel method) in order to quickly calculate the effect a given tail articulation would have on unsteady propeller forces and radiated noise. A small parametric study of sinusoidal tail motions at f = 912 rpm and U = 1 m/s found an amplitude of 2 degrees to be optimal. A 3-dimensional propeller unsteady force simulation was carried out using propeller inflow data from PIV experiments as well as velocity data generated by the reduced order model of tail articulation. This simulation used a "frozen-wake" (quasi-static wake) approximation, which is assumed to be valid because the investigation was limited to non-lifting propeller blades. Both simulated (reduced order model) and measured (PIV) wakes were used as initial conditions in the PUF simulation. Figure 14 shows peak pressures and effective sound pressure levels (ESPL) predicted by the PUF code.

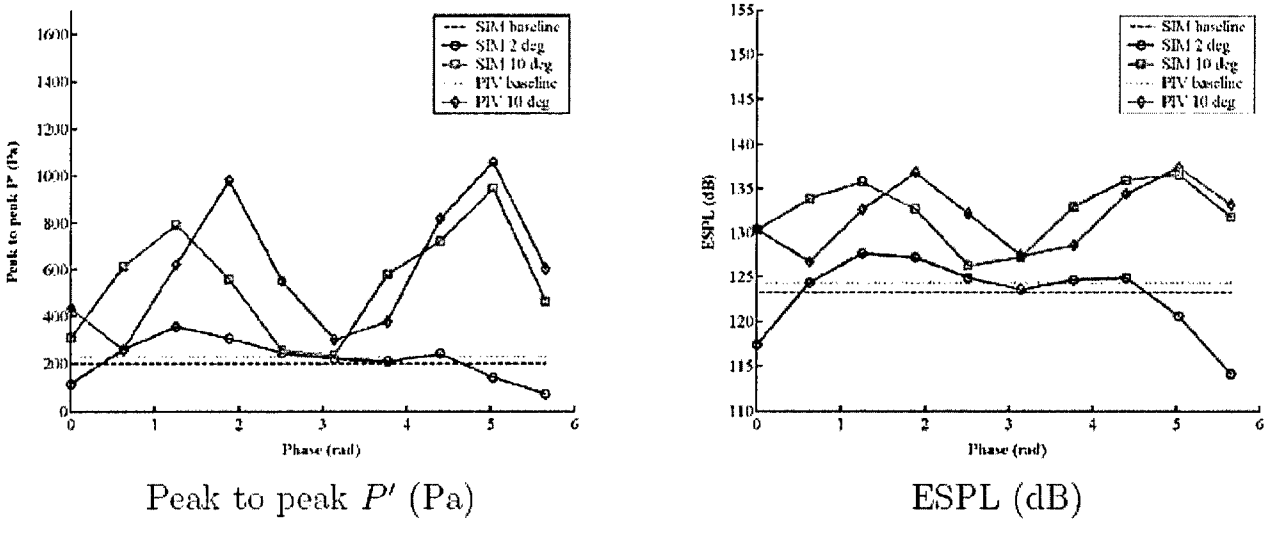

Figure 14 Study of peak to peak P' (Pa) and ESPL (dB) as predicted by PUF with PIV and simulated wakes for varying amplitude and phase

Results from PUF simulations showed that reduction in the effective sound pressure level of radiated noise of up to 5 dB is possible using tail articulation. Estimates of the self induced noise

due to tail articulation showed that the additional noise radiated will most likely be less than the achieved noise reduction.

An interesting point must be made about the sinusoidal tail motion with f = 912 rpm, U = 1 m/s, and A = 2 degrees which was found to best reduce noise radiated in the wake blade interaction. While it is unknown if the *Cd* to *St* relationship in Figure 6 will hold at 2 of amplitude degrees, the current plot shows this case will be a maximum drag wake. This result is interesting in that it runs counter to the original conceptions about tail articulation. It was thought that tail articulation would reduce unsteady blade forces by eliminating the wake deficit behind the stator, which would correspond to $Cd = 0$. However, this result implies that the optimal tail motion for noise reduction incurs the highest effective stator drag. Therefore, reduction in radiated noise may come at the cost of extra drag induced on the vehicle. It is unknown if the relationship between this extra drag penalty and the reduction of noise is meaningful in some way or if it is simply a coincidence in the specific case tested.

IV. Force Measurements

The next step in the project was a force-instrumented propeller study to observe the effect of tail articulation on unsteady propeller forces. This follows the results above where the effect of stator articulation on wake structures and velocity was quantified. Propeller unsteady force simulations were completed using both simulated and empirical stator-generated wakes as boundary/initial conditions. These models and simulations must be corroborated empirically. To that effect when the original stator-wake apparatus was created, it was designed in such a way to allow for expanding of the apparatus to include a force-instrumented propeller.

The design of a force-instrumented propeller apparatus began in January 2005. The technical requirements of the device were:

1. Measure hydrodynamic forces on a propeller placed downstream of an articulating stator.
2. Drive a propeller such that its rotational velocity and phase relative to the oscillating stator could be controlled.
3. Induce little to no upstream disturbances so as to significantly change the effects of the articulating stator on the flow.
4. Be relatively cost-effective and be available for testing in the summer of 2005.

The main driving components of the apparatus were the propeller motor and the multi-axis load cell used to measure hydrodynamic forces. Due to the various budgetary, time and technical constraints presented an AMTI six-axis MC-1 load-cell and a Stoegra water-proof stepper motor were chosen as the main components of the apparatus.

Several machined-aluminum components attached the propeller, shaft, and motor to the load cell. This design ensured that any forces seen at the propeller blade would be detected by the load cell. An aluminum flange was then used to attach the apparatus to an acrylic water tunnel window. The apparatus would be contained within a fairing attached to the tunnel so that the only hydrodynamic forces measured by the load cell would be those generated by the propeller. Several two-bladed propellers were designed so that they would generate zero-lift at certain pre-

determined rotational velocities. These propellers were made using stereo-lithography (SLA) due to the process' low-cost, short lead-time, and relative durability.

During the summer months of 2005 the apparatus was placed inside the NUWC – Newport water tunnel facility (Figure 15). A National Instruments 6220 DAQ card was synchronized with the previously purchased motion-control card so that any measured force data could be exactly linked to propeller and stator position. After numerous tests in the water tunnel several unexpected technical hurdles became apparent. Mechanical vibrations of the apparatus excited by propeller imbalance and hydrodynamic forces created a great deal of noise in the data. Furthermore it was found that the servo motor used to articulate the tail creates high-frequency RF interference which is picked up by the load cell and DAQ equipment. The amplitude of the noise was large enough to drown out relevant data. After some time a decision was made to redesign the apparatus in order to lower the noise floor by both decreasing mechanical and electrical noise as well as increasing the size and number of propeller blades to increase signal magnitude. Tests with larger propellers showed promise in greatly increasing signal strength to measurable levels.

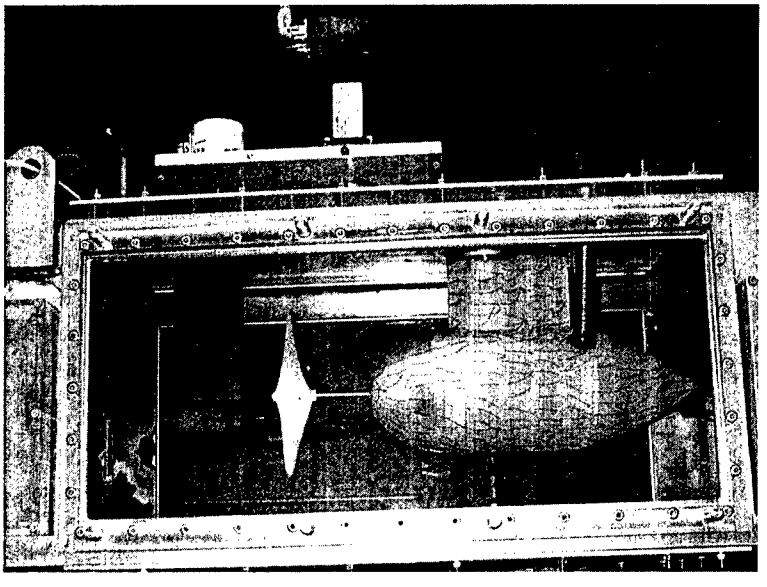

Figure 15: Force measurement apparatus inside SLA fairing.

After numerous tests in the water tunnel several unexpected technical hurdles became apparent. Mechanical vibrations of the apparatus excited by propeller imbalance and hydrodynamic forces created a great deal of noise in the data. Furthermore it was found that the servo motor used to articulate the tail created high-frequency RF interference which is picked up by the load cell and DAQ equipment. The amplitude of the noise was large enough to drown out relevant data. A decision was made to redesign the apparatus in order to lower the noise floor by both decreasing mechanical and electrical noise as well as increasing the size and number of propeller blades to increase signal magnitude.

A new iteration of the propeller force apparatus was designed during the fall of 2005. The new design includes an integrated SLA fairing, larger diameter 3 bladed propellers and a multi-piece motor and bearing support structure that is stronger and stiffer than the previous design. The

intention is to shift mechanical resonance frequencies above the range of frequencies we are interested in measuring and increase the signal to noise ratio of all measurements. In order to deal with the electrical noise problems several steps have been taken such as incorporating torroidal choke inductors and A.C. line filtering to decrease the noise produced by the servo motor and amplifier.

The most challenging aspect of the instrumented-propeller force experiments is measuring the relatively small-scale unsteady forces that result from the interaction between propeller blades and the stator wake. Figure 16 below shows typical propeller-force data comparing a propeller in free-stream to one downstream of a stator. A critical part of the experiment requires accurate measurement of the basic non-articulated stator wake so that any improvements/changes can be compared precisely. Due to various noise sources it was difficult to measure the presence of the stator-wake from propeller force data. Force-data and propeller position was recorded at 2 kHz. The data was then phase-averaged thus removing any noise sources not directly related to propeller rotation. A larger 8" diameter propeller with three blades showed a much cleaner and stronger wake signal than the original 6" two-bladed propeller.

A propeller blade is directly downstream of the stator at angular positions 0°, 120°, and 240°. The no stator cases show some RMS force due to the effects of the downstream load-cell body on the flow-field. While similar data sets for articulating stators have not been collected yet due to electrical noise we have confirmed that with the current hardware, unsteady wake-blade forces can be measure accurately and repeatedly.

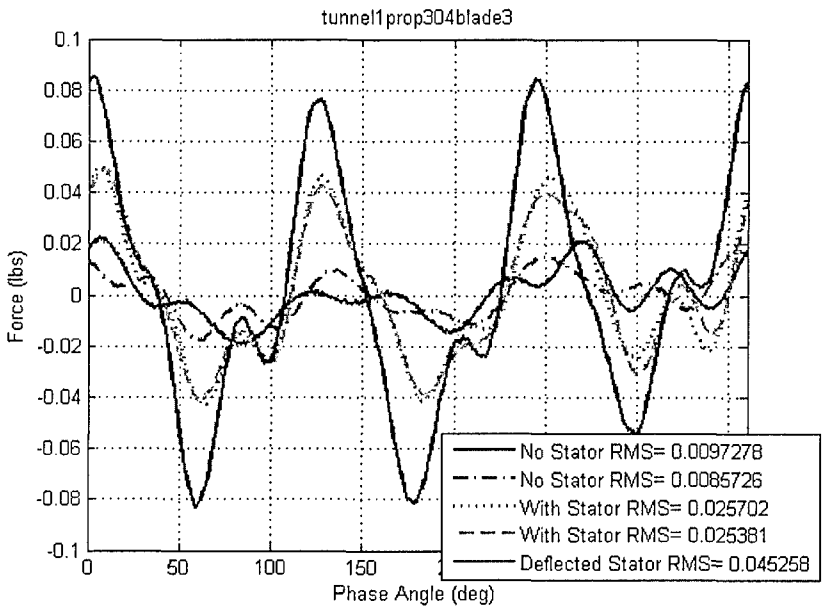

Figure 16: Phase-averaged thrust force versus angular position of a 3-bladed propeller downstream of a stator at NUWC DIV NPT water tunnel (Propeller Speed: 304 RPM, Tunnel Speed: 1m/s)

A new iteration of the propeller force apparatus was designed in FY05 and manufactured during the spring of 2006. The new design included an integrated SLA fairing, larger diameter 3 bladed propellers and a multi-piece motor and bearing support structure that was stronger and stiffer than the previous design. The intention was to shift mechanical resonance frequencies above the range of frequencies we were interested in measuring and increase the signal to noise ratio of all measurements. In order to deal with the electrical noise problems several steps were taken such as incorporating toroidal choke inductors and A.C. line filtering to decrease the noise produced by the servo motor and amplifier.

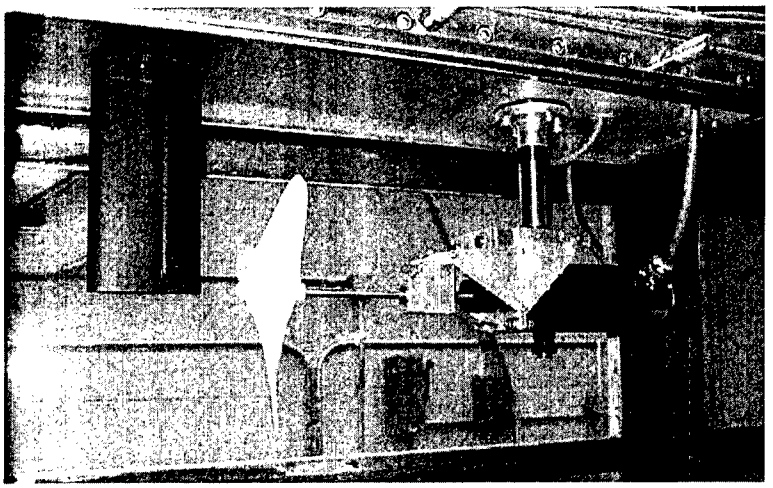

Figure 17: Close up of propeller force measurement apparatus with fairing removed.

An SLA fairing was used to shield the load cell from the surrounding tunnel flow, ensuring that only those forces acting on the propeller blades are measured. Great care was taken so that the fairing was large enough to encase the measurement apparatus with a smooth shape to prevent flow separation. The size of the fairing within the tunnel was critical in order to keep its effect on flow within the test section to a minimum. As Bernoulli predicts, when an ideal fluid within a channel encounters a contraction, flow velocity increased in order to maintain a constant mass transport rate. The fairing creates a blockage in the tunnel so that as water flows around the fairing it is accelerated. In this region of accelerated flow, fluid pressure drops. Since the fairing is a streamlined body in the flow, it also creates a stagnation point at the leading surface. Near this region the flow is decelerated and pressure increases. Therefore the fairing could potentially have a significant effect on the fluid flow field and on propeller forces. For this reason,

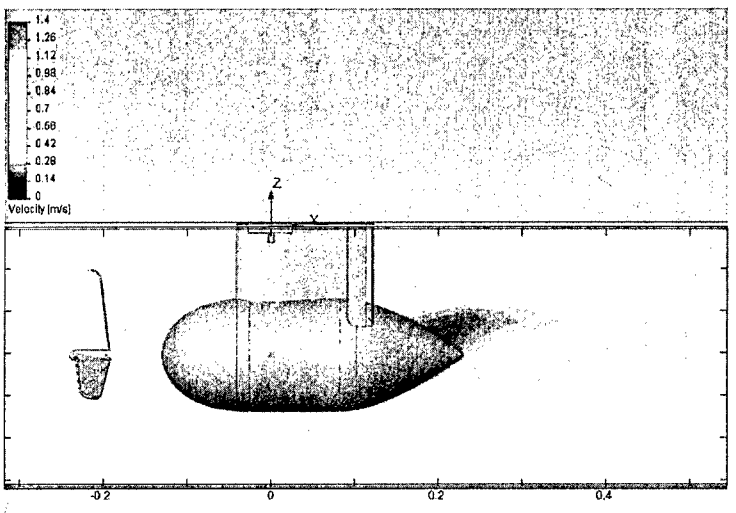

Figure 18: CFD analysis of flow field around fairing. Flow

Computational Fluid Dynamics (CFD) was used to predict the effect of the fairing on the surrounding fluid flow. The fairing shape was modified until CFD results were deemed satisfactory, i.e. negligible effect on the flow field in the vicinity of the propeller. The impact on the surrounding flow field was empirically verified using LDV measurements.

The effect of stator articulation on the instantaneous thrust force generated by two and three bladed propellers versus propeller angular position was measured. Four propellers were tested which were designed to operate in a range of speeds (212-456 RPM in 1 m/s flow). These propellers were designed so that at a certain ratio of flow velocity to rotational velocity they generate no lift. Non-lifting propellers were chosen so that their presence would have as little influence on the stator wake as possible. Stator articulation was controlled so that each propeller blade would encounter an identical wake by fixing the flapping rate to be equal to a particular propeller's blade rate. Experiments were conducted by varying the phase angle and flapping amplitude of stator articulation for each particular propeller.

The effect of stator articulation on the instantaneous thrust force generated by two and three bladed propellers versus propeller angular position was explored. Figure 19 shows the unsteady thrust force generated by each tested propeller when operated within a static stator wake. This work confirms the ability of sinusoidal stator tail articulation to effectively reduce unsteady thrust forces of non-lifting propellers operating within a wake. For a given propeller, the figure shows that the Strouhal number and phase angle of articulation can be specified so that a significant unsteady thrust reduction is accomplished over the baseline static stator wake. Each force peak corresponds to the angular position when a propeller blade is directly downstream of the stator, i.e. in the stator wake. It was hoped that stator articulation would reduce or alter these unsteady forces thus reducing blade tonal noise.

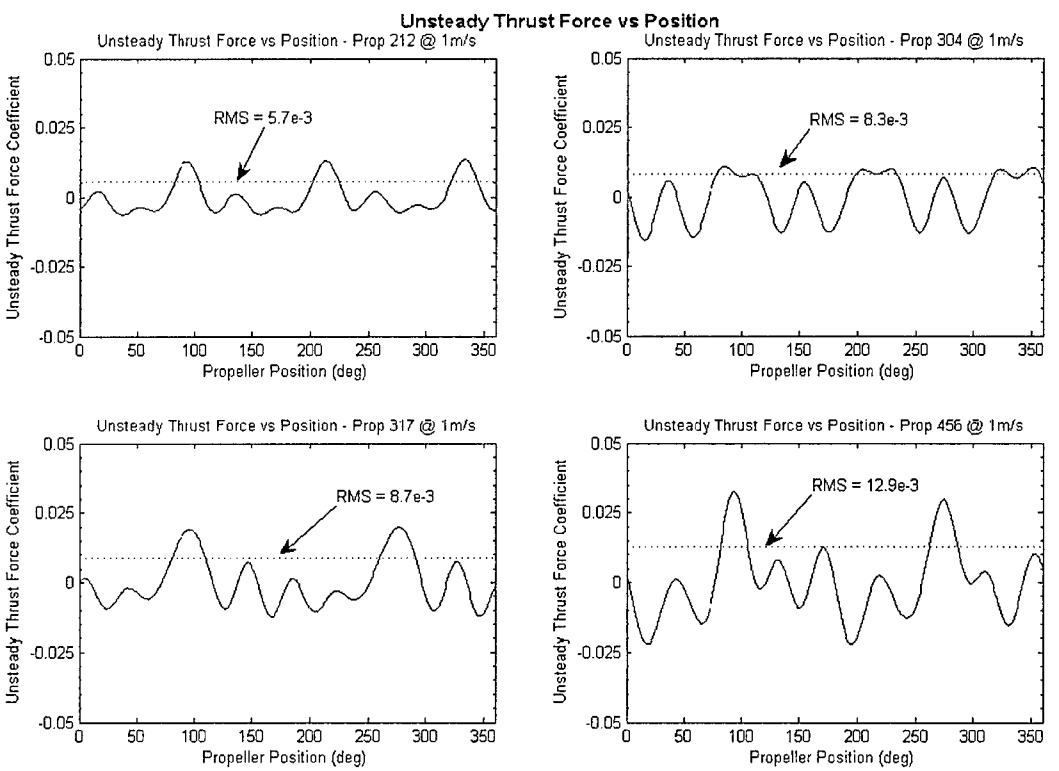

Figure 19: Unsteady Thrust Coefficient vs propeller position for various propellers in a baseline stator wake @ 1m/s

It was found that the unsteady thrust force generated by each propeller was indeed affected by the specific tail articulation tested. Figure 5 shows typical results obtained from one of the propellers studied under sinusoidal tail articulation. As expected, the phase angle between the stator and propeller is one of the factors determining the unsteady noise produced. At a given tail articulation amplitude and rate, the phase angle of the stator controls the configuration of the wake when a blade crosses it. In the case of the test scenario presented in figure 20, at certain phase angles a reduction in the unsteady thrust force occurs. Figure 21 summarizes the results obtained for the propellers tested. In this figure, the root mean square of the time derivative of the unsteady thrust force is presented since that is approximately proportional to radiated tonal noise. It becomes clear, from figure 21, that at for certain flapping scenarios, unsteady forces are reduced but in other cases unsteady thrust increases.

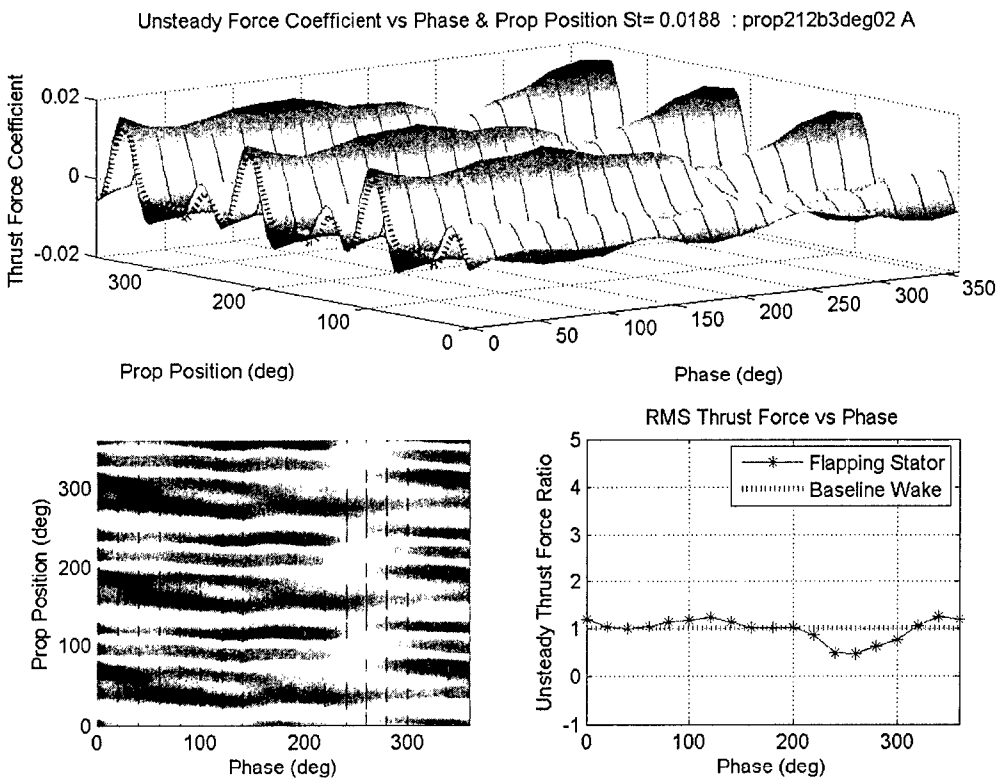

Figure 20: Propeller 212 RPM @ 1m/s, 2 degree flapping amplitude, St = 0.0187 at all phase angles

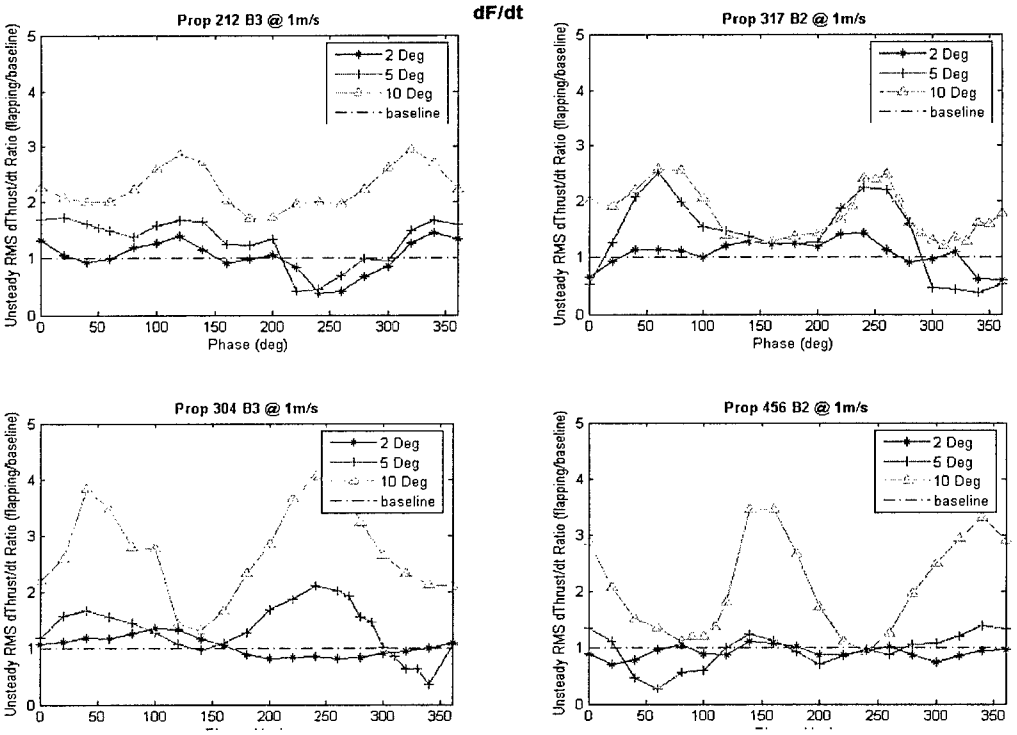

Figure 21: RMS of the time derivative of the thrust force coefficient versus phase for various propellers at different flapping amplitudes

Figures 22 and 23 show the resulting best and worst-case unsteady thrust force measured as a function of the tail Strouhal number. For the propellers tested, stator articulation at a Strouhal number of 0.08 and below was capable of significantly reducing the RMS of both the unsteady thrust force and its time derivative as compared with the baseline wake.

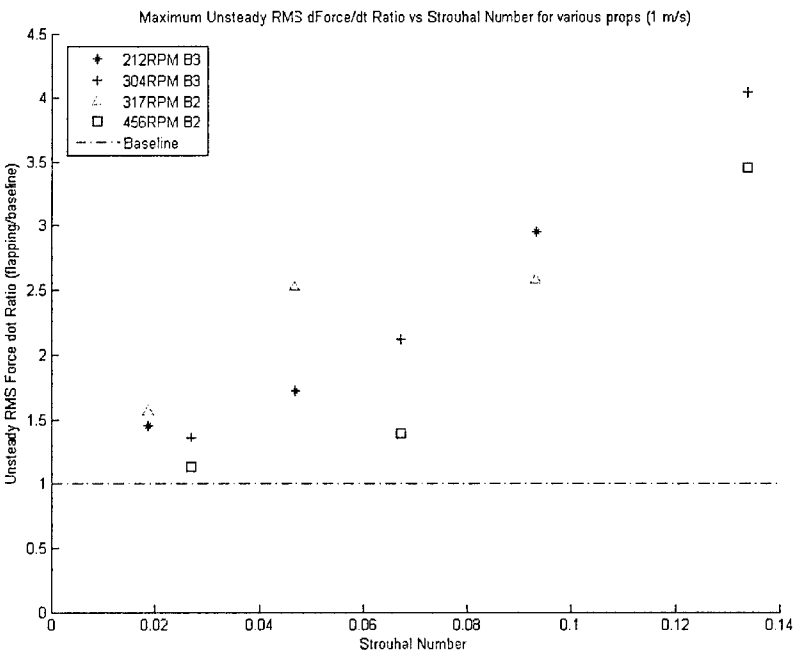

Figure 22: RMS of the maximum unsteady thrust force derivative phase angle case versus Strouhal number. Values less than 1 indicate a reduction over baseline.

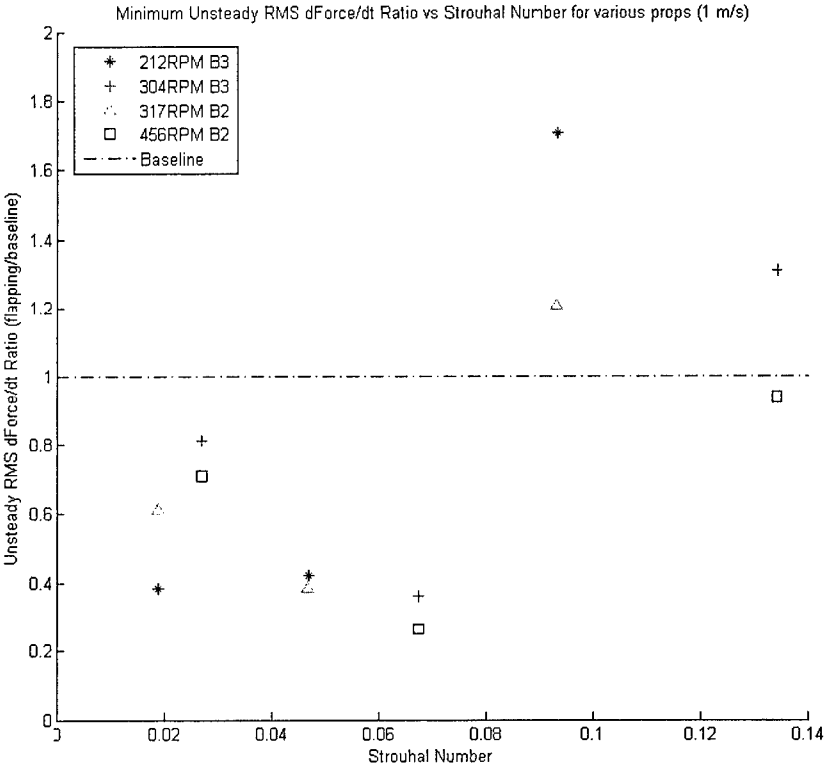

Figure 23: RMS of the minimum unsteady thrust force derivative phase angle case versus Strouhal number. Values less than 1 indicate a reduction over baseline.

At Strouhal numbers above 0.08, stator flapping created increased unsteady thrust forces for every propeller. At all Strouhal numbers tested, certain phase angles generated high unsteady thrust forces, creating the potential of increases unsteady forces and hence noise even when operating at St < 0.08.

Similar results were found when the spectra of the measured thrust force were analyzed. Figure 24 shows typical measured unsteady thrust force spectra. Below St < 0.08 at certain phase angles, articulation was capable of reducing the magnitude of the first several blade harmonics as compared with the baseline case. Certain phase angles of St < 0.08 and all phase angles when operating at St > 0.08 showed an increase in the magnitude of these blade harmonics over the baseline case as seen in figure 24.

The concept of using asynchronous stator flapping was explored. It is believed that articulation of this nature would lead to beating and the unsteady forces generated at certain cycles would be higher than the baseline wake, making it ill-suited for a stealth application.

The relationship between stator flapping phase and unsteady forces was further examined through the use of a reduced order articulation model discussed previously. This two-dimensional model was used to generate a three-dimensional representation of the stator wake flow field. Superposition of an animated 3D propeller model allowed the relative position between propeller blades and wake vortices to be visualized. From these simulations it was found that the phase angles which demonstrated minimum unsteady forces correspond to phases where propeller blades cross the wake between vortices. Conversely, increased unsteady forces corresponded to phase angles where propeller blades 'slice' through wake vortices as they traverse the region directly downstream of the stator. The effect of wake vortices on the velocity field surrounding propeller blades was explored, however it became apparent that only a three dimensional analysis would yield an complete understanding of the relationship between instantaneous propeller forces and relative wake-blade position and vortex strength.

As a final note, in previous work it was hypothesized that the most significant noise reduction occurred at Strouhal numbers corresponding to a maximum drag stator wake. In this work, significant reduction in unsteady forces was seen up to a Strouhal number of 0.08, which corresponds to a stator with a reduced drag wake.

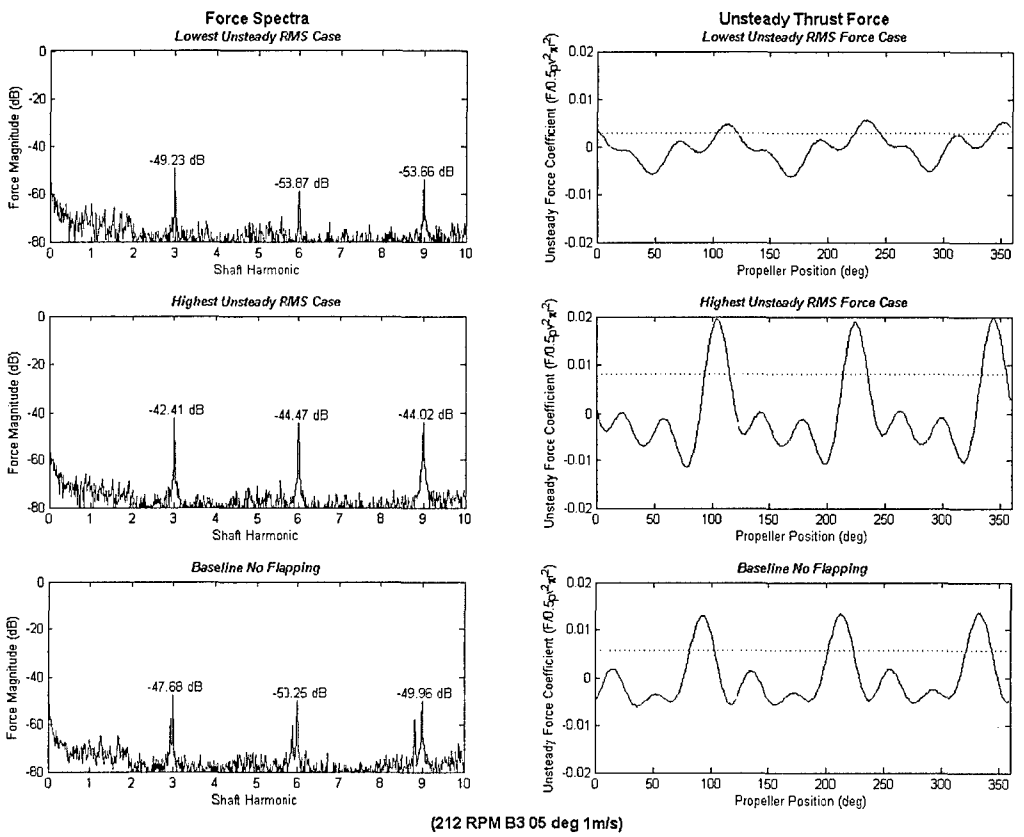

Figure 24: Discrete Fourier Transform of the highest, lowest and baseline RMS thrust force cases for propeller A (212RPM), 5 degree amplitude @ 1m/s

Summary of Key results

1. Designed and built life scale stator with articulating tail section to meet high frequency requirements for use at high Reynolds number.
2. Time mean and phase averaged wake velocity measurements show distinct transition between a quasi-steady region and the beginning of strong vortex rollup as tail Strouhal number is increased. This in turn may have implications on wake deficit reduction and therefore noise alteration.
3. The wake can be characterized by the rollup of an alternating vortex sheet into three distinct regimes based on *Cd* and *St*. PIV visualization shows these distinct regimes.
4. Nonsinusoidal profiles are capable of generating uneven wakes with an increased number of vortices.
5. Reduced order simulations of the wake and blade-vortex interactions were created to aid in a parametric study of the noise reduction potential of various move profiles.
6. 3D PUF simulations were used to predict radiated noise and propellers forces for both simulated and measured wakes.
7. Results from PUF simulations predict that reduction in the effective sound pressure level of radiated noise of up to 5 dB is possible using tail articulation.
8. New propeller force measurement apparatus was designed and manufactured. A multi-piece SLA fairing was incorporated to shield the load cell from measuring extraneous forces. Fairing was designed using CFD so that its impact on the fluid flow would be minimal. Flow around fairing was measured empirically with LDV.
9. Unsteady propeller thrust force due to a propeller operating in an articulation stator wake was measured and compared with the static baseline wake case. For all Strouhal numbers, the relative magnitude of unsteady forces varies with the stator-propeller phase angle and St. RMS unsteady force exhibits local minima and maxima related to phase angle.
10. At St < 0.08 certain phase angles exhibit unsteady force (and the time derivative of unsteady force) reduction compared to the baseline wake. At St > 0.08 unsteady forces are greater than the baseline wake for all phase angles. These cases correspond to a 10 degree flapping amplitude.
11. For all St, the highest unsteady forces produced (corresponding to certain phase angles) are greater than force in the baseline wake and they become larger with increasing St.
12. Unsteady thrust force and its time derivative exhibit the same trends with respect to St, phase, and flapping amplitude.
13. Spectra of unsteady force and its time derivative exhibit changes in the magnitudes of blade rate tonals consistent with changes in measured RMS unsteady force versus St, phase angle and flapping amplitude.
14. 2D reduced-order model was used to calculate velocity field due to stator articulation. Using 3D visualization, relative propeller-wake vortex position was observed to determine effect of instantaneous wake on propeller blade forces.
15. Strength, shape, and separation of wake vortices varied with St. Wake vortex sheet shows increasing roll up with high St.
16. Phase angles showing the lowest RMS unsteady forces correspond to wake blade timing such that propeller blades traverse the gap between vortices. Phase angles exhibiting the

highest RMS unsteady forces correspond to situations where propeller blades 'slice' through wake vortices.

17. 2D analysis of wake velocities at a point on blade leading edge was insufficient in fully describing the effect of the wake on blade forces.

The main conclusions from the proposed research are that strong vortex features can be produced in the presence of tail articulation methods, that these features correspond to about 5-10 db reduction in the blade tonals and that tail-articulation introduced a significant alteration in the unsteady forces experienced by the propulsors over a range of frequencies. These results are expected to be invaluable for future studies of stealth for underwater vehicles.

REFERENCES

1. Macumber, D., "Blade Tonal Noise Reduction Using Tail Articulation at High Reynolds Number," MS Thesis, Massachusetts Institute of Technology, Cambridge, MA, 2005.
2. Macumber, D., "Reduction Of Noise Due To The Stator Wake Blade Interaction By Tail Articulation At High Reynolds Number," *International Symposium on Unmanned Untethered Submersible Technology*, Durham, NH, August 2005. (Best Student Paper Award Winner).
3. Macumber, D., Annaswamy, A., Beal, D. and S. Huyer, "Reduction Of Noise Due To The Stator Wake Blade Interaction By Tail Articulation At High Reynolds Number," *IEEE Journal of Ocean Engineering,* Feb. 2006 (provisionally accepted).
4. James, R., "Reduction of Unsteady Underwater Propeller Forces via Active Tail Articulation," MS Thesis, Massachusetts Institute of Technology, Cambridge, MA, 2006.
5. D. Macumber, D. Beal, A. Annaswamy, C. Henoch, and S. Huyer. "Wake Filling by Active Tail Articulation. Division of Fluid Dynamics", Seattle, WA, November 2004. American Physical Society.
6. A. Annaswamy, D. Macumber, D. Beal, and S. Huyer. "Biomimetic Control of Stator Wake Effects for Blade Tonal Alterations". Active 04, Williamsburg, VA, September 2004. Institute of Noise Control Engineering.